Metabolic Engineering 42 (2017) 175–184

Contents lists available at ScienceDirect

Metabolic Engineering

journal homepage: www.elsevier.com/locate/meteng

The ethanol pathway from *Thermoanaerobacterium saccharolyticum* improves ethanol production in *Clostridium thermocellum*

Shuen Hon[a,c], Daniel G. Olson[a,c,*], Evert K. Holwerda[a,c], Anthony A. Lanahan[a,c], Sean J.L. Murphy[a,c], Marybeth I. Maloney[a,c], Tianyong Zheng[b,c], Beth Papanek[c,d], Adam M. Guss[c,d], Lee R. Lynd[a,b,c,*]

[a] *Thayer School of Engineering, Dartmouth College, Hanover, NH 03755, USA*
[b] *Department of Biological Sciences, Dartmouth College, Hanover, NH 03755, USA*
[c] *Bioenergy Science Center, Oak Ridge National Laboratory, Oak Ridge, TN 37830, USA*
[d] *Biosciences Division, Oak Ridge National Laboratory, Oak Ridge, TN 37830, USA*

ABSTRACT

Clostridium thermocellum ferments cellulose, is a promising candidate for ethanol production from cellulosic biomass, and has been the focus of studies aimed at improving ethanol yield. *Thermoanaerobacterium saccharolyticum* ferments hemicellulose, but not cellulose, and has been engineered to produce ethanol at high yield and titer. Recent research has led to the identification of four genes in *T. saccharolyticum* involved in ethanol production: *adhE*, *nfnA, nfnB* and *adhA*. We introduced these genes into *C. thermocellum* and observed significant improvements to ethanol yield, titer, and productivity. The four genes alone, however, were insufficient to achieve in *C. thermocellum* the ethanol yields and titers observed in engineered *T. saccharolyticum* strains, even when combined with gene deletions targeting hydrogen production. This suggests that other parts of *T. saccharolyticum* metabolism may also be necessary to reproduce the high ethanol yield and titer phenotype in *C. thermocellum*.

1. Introduction

Clostridium thermocellum is a candidate organism for the consolidated bioprocessing of lignocellulosic biomass into biofuels such as ethanol (Olson et al., 2012). It is among the most effective of microorganisms at solubilizing lignocellulose (Lynd et al., 2002; Paye et al., 2016), and is also capable of fermenting the released sugars to organic acids, hydrogen, and ethanol. There have been numerous studies aimed at engineering *C. thermocellum* to produce ethanol as the sole fermentation product at high yield and titer; (Argyros et al., 2011; Biswas et al., 2015, 2014; Deng et al., 2013; Kannuchamy et al., 2016; Papanek et al., 2015; Tian et al., 2016b) these attempts have thus far fallen short of the high yields and titers achieved by conventional ethanol producing organisms such as *Saccharomyces cerevisiae* and *Zymomonas mobilis*.

These engineering attempts in *C. thermocellum* can be grouped into two categories: the first group encompasses strategies that focused on eliminating native competing metabolic pathways, such as organic acid production (Argyros et al., 2011; Biswas et al., 2014; Rydzak et al., 2015) or hydrogen production (Biswas et al., 2015), or a combination thereof (Papanek et al., 2015; Tian et al., 2016b), often coupled with adaptive evolution for faster growth of the engineered strain. Table 1 summarizes the reported ethanol yields and titers of these various engineering attempts; the highest yield and titers observed to date are in strain LL1210, with a maximum yield of 75% and maximum observed ethanol titer of 25 g/L (Tian et al., 2016b). Strain LL1210, however, suffers from a slightly reduced growth rate (Tian et al., 2016b) relative to wild type *C. thermocellum* (Olson et al., 2017).

The second group of engineering attempts has focused on introducing heterologous genes that are a part of well-characterized ethanol producing pathways into *C. thermocellum*; examples include expressing pyruvate kinase (Deng et al., 2013), expressing pyruvate decarboxylase and an alcohol dehydrogenase (Kannuchamy et al., 2016), replacing the native *rnf* operon with *Thermoanaerobacterium saccharolyticum* ferredoxin:NAD^+ oxidoreductase (Tian et al., 2016a), and expressing heterologous bifunctional alcohol dehydrogenases (*adhE*) in an *adhE* deletion strain (Lo et al., 2015a) of *C. thermocellum* (Hon et al., 2016). There has also been an attempt at overexpressing native genes to increase ethanol yield and titer, specifically overexpressing the *rnf* operon in *C. thermocellum* (Lo et al., 2016). Given that the best ethanol yield achieved among these strategies is just over 60% (overexpression of the

* Corresponding authors at: Thayer School of Engineering, Dartmouth College, Hanover, NH 03755, USA.
E-mail addresses: Daniel.G.Olson@dartmouth.edu (D.G. Olson), Lee.R.Lynd@dartmouth.edu (L.R. Lynd).

http://dx.doi.org/10.1016/j.ymben.2017.06.011
Received 21 March 2017; Received in revised form 27 May 2017; Accepted 23 June 2017
Available online 27 June 2017

Table 1
Summary of ethanol yields and titers from several *C. thermocellum* engineering strategies.

Strain name	Description of genetic engineering performed	Maximum yield[a,b] (% theoretical maximum)	Maximum reported titer[a] (g/L)	Reference
AG553	Eliminated organic acid production and hydrogen production; very slow growth rate (μ = 0.06/h)	**78** (1.0 g/L Avicel)	**3.4** (20.0 g/L Avicel)	(Papanek et al., 2015)
LL1210	Adaptive evolution of strain AG553; faster growth rate (μ = 0.22/h)	**75** (60.0 g/L Avicel)	**26.7** (94.9 g/L Avicel)	(Tian et al., 2016b)
AG1150	Elimination of hydrogen production	**64** (5.0 g/L cellobiose)	**1.6** (5.0 g/L Avicel)	(Biswas et al., 2015)
M1570	Eliminated acetic acid and lactic acid production, with adaptive evolution	**60** (19.5 g/L Avicel)	**5.6** (19.5 g/L Avicel)	(Argyros et al., 2011)
CTH-*pdc-adh*	Introduced *Zymomonas mobilis* pyruvate decarboxylase and alcohol dehydrogenase	**53** (10.0 g/L cellobiose; complex medium)	**3.0** (10.0 g/L cellobiose; complex medium)	(Kannuchamy et al., 2016)
LL1275	Hydrogen production reduced; overexpressed *rnf* operon	**65** (4.6 g/L cellobiose)	**5.2** (49.7 g/L Avicel)	(Lo et al., 2016)
LL1113	Replaced native *ldh* with *T. saccharolyticum* pyruvate kinase; deleted malate shunt	**47** (4.6 g/L cellobiose)	**1.2** (4.6 g/L cellobiose)	(Deng et al., 2013)
LL1338	Replaced *rnf* operon with *T. saccharolyticum* NADH-*fnor*	**35** (9.9 g/L cellobiose)	**1.7** (9.9 g/L cellobiose)	(Tian et al., 2016a)

[a] Parentheses after the values indicate the substrate and its initial concentration at which the value was observed.
[b] The maximum theoretical yield assumes two molecules of ethanol can be produced from one molecule of glucose (or equivalent).

rnf operon, Table 1), there is room for further improvement.

T. saccharolyticum has been previously engineered for high ethanol yield and titer (Herring et al., 2016; Shaw et al., 2012, 2008). Recent work has identified four proteins that are important for the high ethanol yield phenotype in one of these engineered strains of *T. saccharolyticum*, M1442 (Herring et al., 2016): an AdhE that contains a G544D mutation in the protein and that has NADPH-linked acetaldehyde dehydrogenase (ALDH) activity (Zheng et al., 2015), the NADH-dependent reduced ferredoxin:$NADP^+$ oxidoreductase complex, NfnAB (i.e. a complex of the NfnA and NfnB proteins) (Lo et al., 2015b), and an NADPH-dependent alcohol dehydrogenase, AdhA (Zheng et al., 2017).

In this study, we hypothesized that expressing key genes of the *T. saccharolyticum* pathway in *C. thermocellum* might result in improved ethanol production. To test this, we expressed the *T. saccharolyticum* $adhE^{G544D}$, *nfnAB*, and *adhA* genes (Fig. 1) from strain M1442 (Herring et al., 2016), either individually or in combination, into wild type *C. thermocellum*, and determined ethanol yield and titer on both soluble carbon sources and high loadings of crystalline cellulose.

2. Materials and methods

2.1. Strain and plasmid construction

Table 2 lists the strains used and constructed in this study, as well as the plasmids used for integrating and deleting genes of interest and expression plasmids (Hon et al., 2016) built and used in this study. Plasmids were constructed via the isothermal assembly reaction (Gibson, 2011) using a commercial kit sold by New England Biolabs (NEBuilder® HiFi DNA Assembly Master Mix, catalog number E2621). DNA purification of plasmid DNA or PCR products for cloning was performed using commercially available kits from Qiagen, Zymo Research, or New England Biolabs. *C. thermocellum* strains were transformed using previously described methods (Olson and Lynd, 2012a); all plasmid DNA destined for transforming into *C. thermocellum* was propagated and purified from *Escherichia coli* BL21 derivative strains (New England Biolabs catalog number C2566) to ensure that the DNA was properly methylated (Guss et al., 2012).

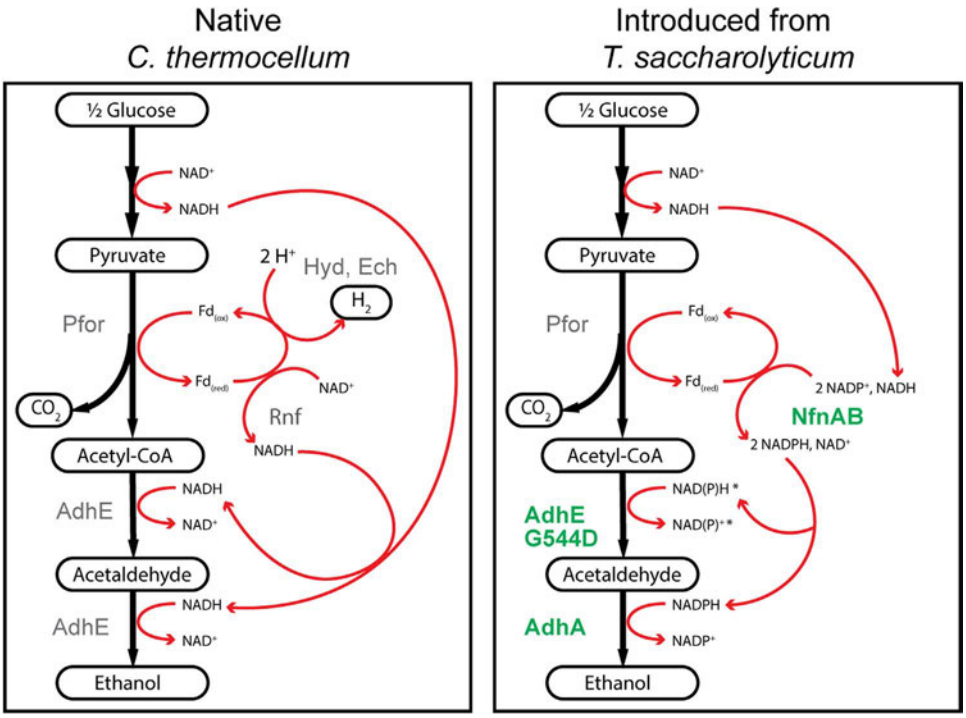

Fig. 1. Conversion of ½ glucose to ethanol via the native *C. thermocellum* pathway or the introduced *T. saccharolyticum* pathway; pathways leading to organic acid production have been excluded for simplicity. Black arrows represent carbon flux, red arrows represent electron flux. Proteins that play a role in ethanol formation are named in grey; the *T. saccharolyticum* proteins that are introduced into *C. thermocellum* in this study are named in green. * See Section 3.3. (For interpretation of the references to color in this figure legend, the reader is referred to the web version of this article)

Table 2
List of strains and integration/deletion plasmids used in this study.

Strains/Plasmids	Organism	Description	Accession number	Reference or source
E. coli T7 express	*Escherichia coli*	*fhuA2 lacZ::T7 gene1 [lon] ompT gal sulA11 R(mcr-73::miniTn10–TetS)2 [dcm] R(zgb-210::Tn10–TetS) endA1 Δ(mcrC-mrr)114::IS10*		New England Biolabs (Ipswich, MA)
E coli T7 Express *lysY/I^q*	*E. coli*	*MiniF lysY lacI^q(Cam^R) / fhuA2 lacZ::T7 gene1 [lon] ompT gal sulA11 R(mcr-73::miniTn10–Tet^S)2 [dcm] R(zgb-210::Tn10–Tet^S) endA1 Δ(mcrC-mrr) 114::IS10*		New England Biolabs (Ipswich, MA)
LL1375	*E. coli*	*E. coli* T7 Express *lysY/I^q*with plasmid expressing wild type *T. saccharolyticum adhE*		(Zheng et al., 2015)
LL1376	*E. coli*	*E. coli* T7 Express *lysY/I^q*with plasmid expressing *T. saccharolyticum adhE^{G544D}*		(Zheng et al., 2015)
M1442	*T. saccharolyticum*	Engineered and evolved *T. saccharolyticum*	SRA233073	(Herring et al., 2016)
LL1004	*C. thermocellum*	DSM 1313	CP002416	DSMZ
AG929	*C. thermocellum*	DSM1313 *Δhpt ΔClo1313_0478*	SRP097241	This study
LL1319	*C. thermocellum*	AG929 P$_{Clo1313_2638}$::*adhA*(*Tsc*)-*nfnAB*(*Tsc*)-*adhE*^{G544D} (*Tsc*)		This study
LL1323	*C. thermocellum*	LL1319 *ΔadhE* (*Clo1313_1798*)	SRP097238	This study
LL1324	*C. thermocellum*	LL1319 *Δech* (*Clo1313_0570-Clo1313_0575*)	SRP097237	This study
LL1325	*C. thermocellum*	LL1319 *ΔhydG* (*Clo1313_1571*)	SRP097437	This study
LL1381	*C. thermocellum*	LL1325 *Δech*		This study
LL1390	*C. thermocellum*	AG929 P$_{Clo1313_2638}$::*adhA*(Tsc)-*nfnAB*(Tsc)		This study
LL350	*C. thermocellum*	DSM 1313 *Δhpt ΔhydG*		(Biswas et al., 2015)
AG1150	*C. thermocellum*	DSM 1313 *Δhpt ΔhydG Δech*		(Biswas et al., 2015)
LL1011	*C. thermocellum*	DSM 1313 *Δhpt Δldh Δpta-ack*		(Argyros et al., 2011)
LL1251	*C. thermocellum*	DSM1313 *Δhpt Δldh::P$_{eno}$-pyk*(Tsc) *Δme-mdh Δppdk Δpeps*		(Olson et al., 2017)
pAMG275		*ech* markerless deletion vector		(Biswas et al., 2015)
pAMG278		*hydG* markerless deletion vector		(Biswas et al., 2015)
pJLO19		C. *thermocellum adhE* markerless deletion vector	KP636798	(Lo et al., 2015a)
pDGO145		Deletion/Integration vector backbone	KY852359	This study
pSH074		Integration vector; introduces *T. saccharolyticum adhA-nfnAB-adhE^{G544D}* downstream of the *Clo1313_2638* promoter region	KY852357	This study
pSH075		Integration vector; introduces *T. saccharolyticum adhA-nfnAB* downstream of the *Clo1313_2638* promoter region	KY852358	This study
pDGO143		*C. thermocellum* expression vector	KX259110	(Hon et al., 2016)
pSH062		pDGO143 with *Clo1313_2638* promoter driving *T. saccharolyticum adhE^{G544D} - nfnAB - adhA*	KY820846	This study
pSH063		pDGO143 with *Clo1313_2638* promoter driving *T. saccharolyticum adhE^{G544D} - adhA*	KY820847	This study
pSH064		pDGO143 with *Clo1313_2638* promoter driving *T. saccharolyticum nfnAB - adhA*	KY820848	This study
pSH065		pDGO143 with *Clo1313_2638* promoter driving *T. saccharolyticum adhE^{G544D} - nfnAB*	KY820849	This study
pSH066		pDGO143 with *Clo1313_2638* promoter driving *T. saccharolyticum adhE^{G544D}*	KY820850	This study
pSH067		pDGO143 with *Clo1313_2638* promoter driving *T. saccharolyticum nfnAB*	KY820851	This study
pSH068		pDGO143 with *Clo1313_2638* promoter driving *T. saccharolyticum adhA*	KY820852	This study
pSH069		pDGO143 with *Clo1313_2638* promoter driving *T. saccharolyticum adhE^{G544D} - adhA - nfnAB*	KY820853	This study
pSH070		pDGO143 with *Clo1313_2638* promoter driving *T. saccharolyticum nfnAB - adhE^{G544D} - adhA*	KY820854	This study
pSH071		pDGO143 with *Clo1313_2638* promoter driving *T. saccharolyticum nfnAB - adhA - adhE^{G544D}*	KY820855	This study
pSH072		pDGO143 with *Clo1313_2638* promoter driving *T. saccharolyticum adhA - adhE^{G544D} - nfnAB*	KY820856	This study
pSH073		pDGO143 with *Clo1313_2638* promoter driving *T. saccharolyticum adhA - nfnAB - adhE^{G544D}*	KY820857	This study

2.2. Media preparations and culture conditions

All reagents used in this study were of molecular grade, and obtained either from Sigma Aldrich or Fisher Scientific, unless otherwise noted. *C. thermocellum* strains were grown at 55 °C under anaerobic conditions, either in conical tubes in anaerobic chambers (Coy Laboratory Products, Grass Lakes, MI, USA) with the hydrogen concentrations in the anaerobic chamber maintained at a minimum of 1.5%, or in sealed 150 mL serum bottles that were prepared and inoculated as previously described (Zheng et al., 2017). Complex medium CTFÜD (Olson and Lynd, 2012a) was used to culture *C. thermocellum* cells used either as competent cells in transformations, or for harvesting genomic DNA for strain re-sequencing. Defined MTC-5 medium with the initial pH adjusted to 7.4 was used for all other purposes; the media formula (minus the carbon source) is presented in Supplementary information Table S2. Where cellobiose was the carbon source in MTC-5 medium, it was either used at a concentration of 5 g/L for routine culture, or at 20 g/L for fermentation end product analyses. Where necessary, thiamphenicol (dissolved in dimethyl sulfoxide) was added to the medium to a final concentration of 6 μg/mL. Culture conditions for 1 L bioreactor batch fermentations with high crystalline cellulose (Avicel) loadings under pH-controlled conditions are discussed in Section 2.5.

Specific growth rates were determined as previously described (Olson and Lynd, 2012b).

2.3. Enzyme assays

2.3.1. Preparation of cell extracts

Cell extracts were obtained as previously described (Lo et al., 2015b; Tian et al., 2016a; Zheng et al., 2017, 2015); all steps were performed in Coy anaerobic chambers. *C. thermocellum* strains were grown in MTC-5 with 5 g/L cellobiose as the carbon source to mid-exponential phase (OD_{600} between 0.6 and 1.0) before being harvested; cells were pelleted and the supernatant decanted, before being stored at −80 °C prior to use. Cell pellets were re-suspended in 100 mM Tris-HCl buffer (pH 7.5 at 55 °C), then incubated with 1U of Ready-Lyse lysozyme (Epicenter Biotechnologies, Madison, WI, USA) for 20 min at room temperature. DNase I was then added to the lysed cells, and the mixture was further incubated for 10 min to reduce the viscosity of the cell extract. Cell debris was pelleted by centrifuging at > 12,000 g for 5 min; the supernatant was kept as cell-free extract. Protein concentration of the cell-free extract was determined using Bio-rad (Hercules, CA, USA) protein dye assay reagent, with bovine serum albumin

(Thermo Scientific) used as a standard.

2.3.2. Enzyme assay conditions

All enzyme assay reactions were performed at 55 °C and pH 7.0 under anaerobic conditions in a Coy Anaerobic chamber (Coy Laboratory Products, Grass Lakes, MI).

Alcohol dehydrogenase (ADH) and acetaldehyde dehydrogenase (ALDH) activities were determined as previously described (Zheng et al., 2017, 2015); ADH and ALDH assay reactions were carried out in a reaction mixture containing 100 mM Tris-HCl pH 7.5, 5 μM $FeSO_4$, 0.2 mM NAD(P)H, and cell extract, with the reaction started by the addition of acetaldehyde for the ADH reaction or acetyl-CoA for the ALDH reaction to final concentrations of 20 mM and 3 mM respectively for acetaldehyde and acetyl-CoA (Zheng et al., 2015). For the ALDH assay, we also added $MgCl_2$ to a final Mg^{2+} concentration of 5 mM (Zheng et al., 2014).

Benzyl viologen reduction with NAD(P)H (NAD(P)H:BV) activities were performed as previously described (Lo et al., 2015b; Tian et al., 2016a).

The final volume for all biochemical assays was 1200 μL.

2.3.3. Assay for ethanol production

Ethanol production assays were performed using defined MTC-5 medium as previously described (Hon et al., 2016), with the only difference being an increase in the initial cellobiose concentration from 5 g/L to 20 g/L. Briefly, cultures for the ethanol assays were inoculated with 2% inoculum, and then grown anaerobically at 55 °C for 96 h to ensure complete consumption of available cellobiose. The cultures were pelleted by centrifuging at > 20,000 g for 5 min, and the supernatant was used in the assays; 10 μL of sample was used in a 200 μL reaction volume, with the assay conditions and quantification of ethanol concentrations performed as previously described (Hon et al., 2016).

2.3.4. Protein purification

AdhE protein was purified from *E. coli* as previously described (Zheng et al., 2015).

2.4. Measuring gene expression

Gene expression was measured via reverse transcription quantitative real-time PCR (RT-qPCR), and was done as previously described (Hon et al., 2016). Cultures were grown on defined MTC-5 medium to mid-exponential phase (OD_{600} between 0.6 and 1.0); cultures were then treated with RNAprotect Bacteria Reagent (Qiagen catalog number 76506) per kit instructions, then stored at −20 °C until further use (Hon et al., 2016). Cell lysis, RNA purification, and cDNA synthesis were performed as previously described (Lo et al., 2016; Zhou et al., 2015); the primers used for qPCR are listed in Table S1. Gene expression in all strains were normalized against *C. thermocellum recA* expression (Livak and Schmittgen, 2001) to allow for comparison across strains, as previously done (Hon et al., 2016; Lo et al., 2016; Zhou et al., 2015).

2.5. High solids fermentations

Bioreactor experiments were prepared as previously described (Holwerda et al., 2014), and carried out with an initial working volume of 1 L. MTC-5 was used with 60 g/L crystalline cellulose (Avicel PH105) as carbon source. Bioreactors were inoculated with 10 mL of overnight grown culture on 5 g/L Avicel PH105 in defined MTC-5 medium (1% v/v). pH was maintained at 7.00 ± 0.05 by automatic addition of 4 N KOH.

2.6. Analytical methods

Fermentation products were measured by high pressure liquid chromatography (HPLC) as previously described (Holwerda et al., 2014). Residual cellulose (Avicel PH105) concentration was determined via quantitative saccharification, as previously described (Holwerda et al., 2012). Pellet nitrogen as proxy for cell biomass was measured as previously described (Holwerda et al., 2013, 2012).

2.7. Sequencing and resequencing

Routine Sanger sequencing was performed by Genewiz. Inc. with at least two-fold coverage of coding sequences and promoter regions; whole genome resequencing of strains was performed by the Department of Energy Joint Genome Institute using the Illumina Miseq sequencing platform with an average of 100-fold coverage. Sequencing data was analyzed with the CLC Genomics Workbench version 9.5.4 (Qiagen Inc.), as previously described (Lo et al., 2016; Tian et al., 2016b). Accession numbers for strains and plasmids are listed in Table 2.

3. Results

3.1. Optimizing the synthetic ethanol producing operon

To determine the importance of the *T. saccharolyticum adhA*, *nfnAB*, and *adhE*^{G544D} genes for improved ethanol production in *C. thermocellum*, we constructed plasmids expressing these genes of interest either individually, or in various combinations, using synthetic operons where more than one gene was being expressed (Table 2), and introduced these plasmids into wild type *C. thermocellum* (DSM 1313). When the genes of interest were expressed individually, only *adhA* expression resulted in an improvement of ethanol production in wild type *C. thermocellum* (Fig. 2A); expressing *nfnAB* and *adhE*^{G544D} individually did not have a significant effect on ethanol production in wild type *C. thermocellum*. The observation that all strains with improved ethanol production included *adhA* as one of the genes expressed (Fig. 2A) is consistent with *adhA* being an essential gene for high ethanol yield in *T. saccharolyticum* (Zheng et al., 2017).

We also observed that *nfnAB* improved ethanol production only when it was paired with either *adhA* or *adhE*^{G544D}, with the *adhA-nfnAB* pairing appearing to produce, on average, more ethanol than the *adhE-nfnAB* pairing (Fig. 2A). It appears that expressing *adhA*, *nfnAB*, and *adhE*^{G544D} simultaneously shows no benefit beyond the expression of *adhA* and *nfnAB* (Fig. 2A, pSH062 versus pSH064; p-value = 0.124); however, re-sequencing of some of the improved ethanol producing strains that contained plasmid pSH064 revealed secondary mutations elsewhere in the organism that may have compensated for their lack of *adhE*^{G544D} (data not shown). We therefore sought alternate means of determining the importance of *T. saccharolyticum adhE*^{G544D} for improving ethanol production in *C. thermocellum* in subsequent experiments (see Section 3.3).

The four *T. saccharolyticum* genes being studied were expressed in a synthetic operon (Espah Borujeni et al., 2014; Salis et al., 2009) driven by the strong *Clo1313_2638* promoter (Olson et al., 2015a); we therefore investigated whether the order of gene transcription in the synthetic operon had any effect on ethanol production. Expression plasmids that covered all 6 possible combinations of gene orders (we kept both the A and B subunits of *T. saccharolyticum nfnAB* in their native configuration to simplify the experimental design) (Table 1) were constructed and introduced into wild type *C. thermocellum*. We observed that ethanol production improved as *adhA* was moved closer to the 5′ end (i.e. start) of the operon (Fig. 2B). Where *adhA* was the first gene to be transcribed, it was observed that the order of transcription of *nfnAB* and *adhE*^{G544D} did not result in any significant differences to ethanol production (Fig. 2B, pSH072 versus pSH073; p-value = 0.832). The results also support the secondary importance of *nfnAB*; where *nfnAB* was the first genes to be transcribed, having *adhA* be expressed first resulted in better ethanol production than if *adhE*^{G544D} was the second

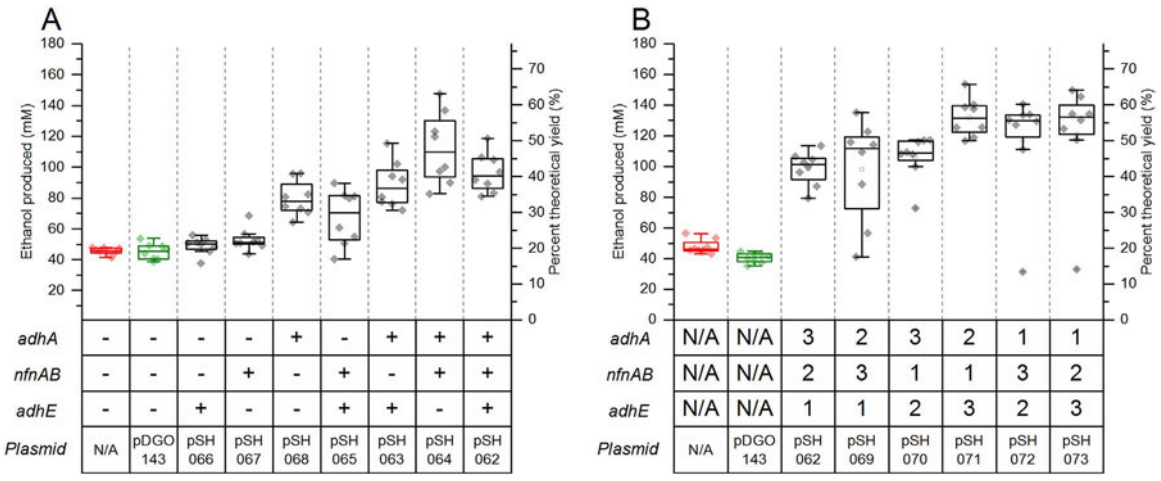

Fig. 2. Ethanol production (as measured using the ethanol production assay) from wild type *C. thermocellum* (strain LL1004) strains grown on MTC-5 with 20 g/L (59 mM) initial cellobiose for 96 h, with 6 μg/mL thiamphenicol added where plasmids are present; the color of the box plots indicate whether a strain contains either no plasmid (red), an empty vector pDGO143 (green), or an expression plasmid (black). 8 colonies were evaluated for each condition; data for each colony is represented by a single point, and was measured in biological replicate (n = 2 for A and n = 3 for B; error bars not shown on individual data points for clarity). The box includes the 25th to 75th percentile of data; whiskers represent 1.5 times the interquartile range. Ethanol was measured via the plate based assay (see Section 2.3.3); the ethanol yield assumes that all cellobiose was consumed. **A.** Determining the importance of the *T. saccharolyticum* genes; "+" and "-" signs indicate whether a *T. saccharolyticum* gene is expressed in a given set of strains. The order of genes is *adhE*^{G544D}-*nfnAB*-*adhA*. **B.** Determining the effect of order of gene expression on ethanol production; numbers under each box plot indicate the order of the gene in the synthetic operon. (For interpretation of the references to color in this figure legend, the reader is referred to the web version of this article)

gene to be expressed (Fig. 2B, pSH070 versus pSH071; p-value = 0.002). These observations further support our hypothesis that *adhA* is the most important gene for improving ethanol production, followed by *nfnAB* and then *adhE*^{G544D}. Based on these results, we determined that the optimal configuration for our *T. saccharolyticum* ethanol production operon was to express the genes in the order *adhA-nfnAB-adhE*^{G544D}.

3.2. Expressing the T. saccharolyticum ethanol production operon in engineered strains of C. thermocellum

Introducing the *T. saccharolyticum* ethanol production operon resulted in a significant increase to ethanol production in wild type *C. thermocellum*; however, the highest achieved yield of about 55% (Fig. 2) is below the threshold of 90% that is commonly thought to be important for industrial ethanol production (Dien et al., 2003), and which has been achieved in other thermophilic bacteria (Olson et al., 2015b), including *T. saccharolyticum* (Herring et al., 2016). We hypothesized that combining the *T. saccharolyticum* ethanol production operon with existing engineered strains would result in higher ethanol yields. We transformed several engineered strains of *C. thermocellum* with expression plasmid pSH062 (Table 1, transformed into strains LL350, AG1150, LL1011, and LL1251); however, the introduction of plasmid pSH062 into these strains did not lead to improvements in ethanol production (Fig. S1).

One possible explanation for the lack of effect of introducing plasmid pSH062 is the acquisition of secondary mutations during the construction of those strains. Therefore, we pursued a strategy of first integrating the heterologous genes from *T. saccharolyticum* into the chromosome of wild type *C. thermocellum*, and then deleting the native competing metabolic pathways.

3.3. Integrating the T. saccharolyticum ethanol operon into C. thermocellum

Strain AG929 (DSM 1313 *Δhpt ΔClo1313_0478*) was chosen as our starting point for gene integrations, as a native restriction system has been deleted, which we reasoned would improve our genetic engineering throughput. Strain LL1319 was created from strain AG929 by integrating the *T. saccharolyticum* ethanol production operon (*adhA*, *nfnAB*, and *adhE*^{G544D}) using plasmid pSH074 (Table 1) such that it was transcriptionally driven by the *Clo1313_*2638 promoter (Olson et al., 2015a) on the chromosome (Fig. S2). We also introduced the ethanol producing operon without *T. saccharolyticum adhE*^{G544D} using plasmid pSH075 (Table 1) to create strain LL1390, with the aim of better determining the effect the mutant *T. saccharolyticum adhE*^{G544D} has on ethanol production.

To verify that the introduced *T. saccharolyticum* genes were expressed and that their respective proteins were functional, we measured both relative gene expression levels (Fig. 3), and assayed cell extracts of strain LL1319 for a gain in the respective enzyme activities (Fig. 4). All of the introduced genes were observed to be expressed (Fig. 3), and we readily detected in cell extracts of LL1319 a gain of NADPH-ADH activity, attributable to the AdhA protein (Zheng et al., 2017), as well as a significant increase in NADPH:BV-linked activity, which we can attribute to the *T. saccharolyticum* NfnAB complex (Lo et al., 2015b) since the *C. thermocellum nfnAB* gene is not highly expressed (Lo et al., 2016) in the wild type, and NADPH:BV activity in wild type *C. thermocellum* is low (Fig. 4).

We did not detect NADPH-ALDH activity which would have been expected from the *T. saccharolyticum* AdhE G544D (Zheng et al., 2015). We reasoned, however, that the *T. saccharolyticum* AdhE G544D protein had to be functional as we were able to delete the *C. thermocellum adhE* in strain LL1319, and still observe ethanol being produced in the resulting strain, LL1323 (Fig. 5), suggesting that there was still ALDH activity in strain LL1323 even after the only native source of ALDH activity was removed (Lo et al., 2015a).

We found that the addition of 5 mM final concentration of Mg^{2+} to the assay reaction allowed detection of NADH-ALDH activity in strain LL1323 (Fig. 4) but no NADPH-ALDH activity, which contradicts previous reports. To resolve this anomaly, both *T. saccharolyticum* wild type AdhE and AdhE G544D were purified from *E. coli*, and their ALDH cofactor specificities were measured with or without 5 mM Mg^{2+} added to the assay reaction. Similar to previous results (Zheng et al., 2015), we observed some amount of ALDH activity without 5 mM Mg^{2+}: wild-type AdhE had NADH-linked activity and AdhE G544D had NAPDH-linked activity. Upon addition of 5 mM Mg^{2+}, we saw a greater than four-fold increase in NADH-linked ALDH activity in both AdhE enzymes, while NADPH-linked ALDH activity remained the same (Fig. S3). Thus Mg^{2+} appears to be an important activator for the AdhE protein from *T. saccharolyticum*.

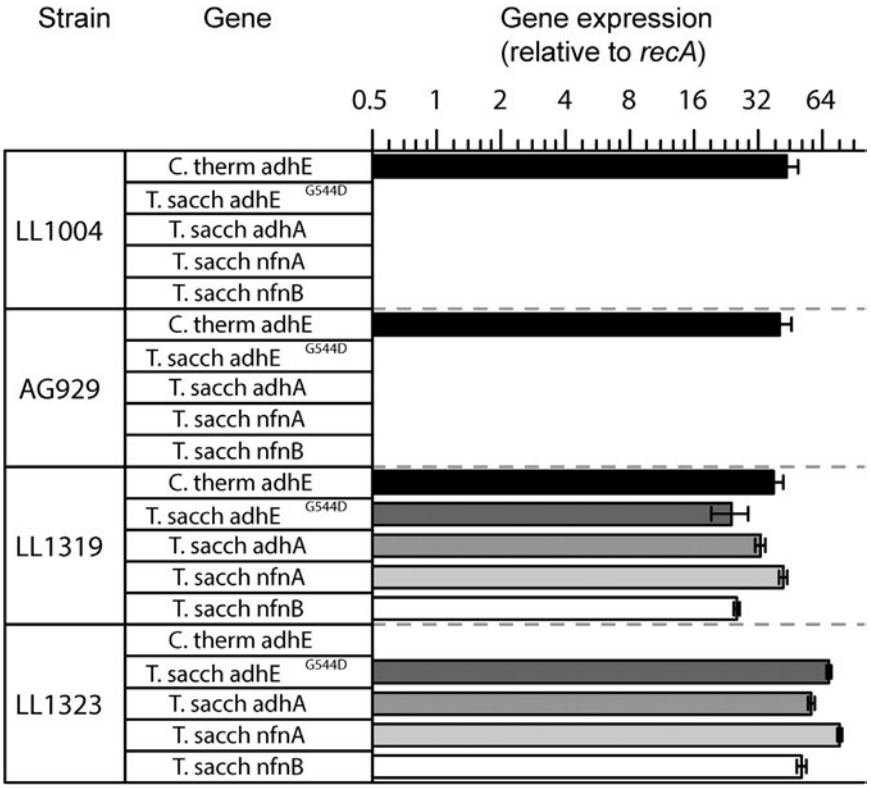

Fig. 3. Relative expression levels (normalized against *C. thermocellum recA* expression) of *C. thermocellum adhE* and the introduced *T. saccharolyticum* genes. Error bars represent one standard deviation (n = 3).

3.4. Fermentation analyses of the engineered C. thermocellum strains

We observed similar improvements to ethanol production as a result of introducing the *T. saccharolyticum* ethanol production operon (*adhA*, *nfnAB*, and *adhE*^{G544D}: strain LL1319), either with an expression plasmid or by integrating the genes onto the chromosome. The latter method led to a significant increase in ethanol yield on 19 g/L cellobiose, achieving 74% of theoretical maximum (Fig. 5). To determine the effect of the *T. saccharolyticum adhE*^{G544D} gene, another strain was constructed, similar to LL1319, but lacking the *T. saccharolyticum adhE*^{G544D} gene (see Section 3.3). The lack of *T. saccharolyticum adhE*^{G544D} was associated with a decrease in ethanol yield and titer (Fig. 5), suggesting that it does, in fact, play a role in strain LL1319. However, it appears that ethanol production is still dependent on the native AdhE protein, as deleting it from strain LL1319 to create strain LL1323 led to a significant decrease in both the ethanol titer and yield (Fig. 5B).

Hydrogen production was decreased or effectively eliminated in strain LL1319 by deleting either or both the hydrogenase maturase gene, *hydG*, and the [NiFe] hydrogenase complex, *ech* (Biswas et al., 2015). It was previously shown that eliminating hydrogen production via these two gene deletions led to a greater improvement in ethanol yield than eliminating acetic acid and lactic acid production (Argyros

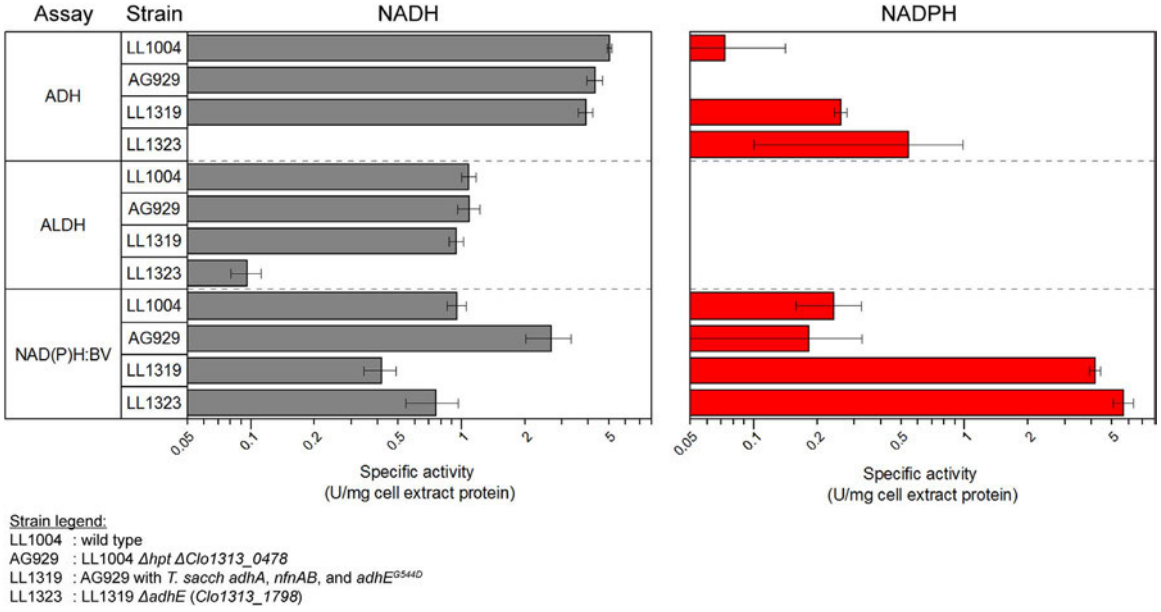

Fig. 4. Specific activities for the alcohol dehydrogenase (ADH), acetaldehyde dehydrogenase (ALDH) and NAD(P)H:BV activities. 1 unit of activity (U) is equivalent to the formation of 1 μmol of product per minute. Error bars represent one standard deviation (n = 3).

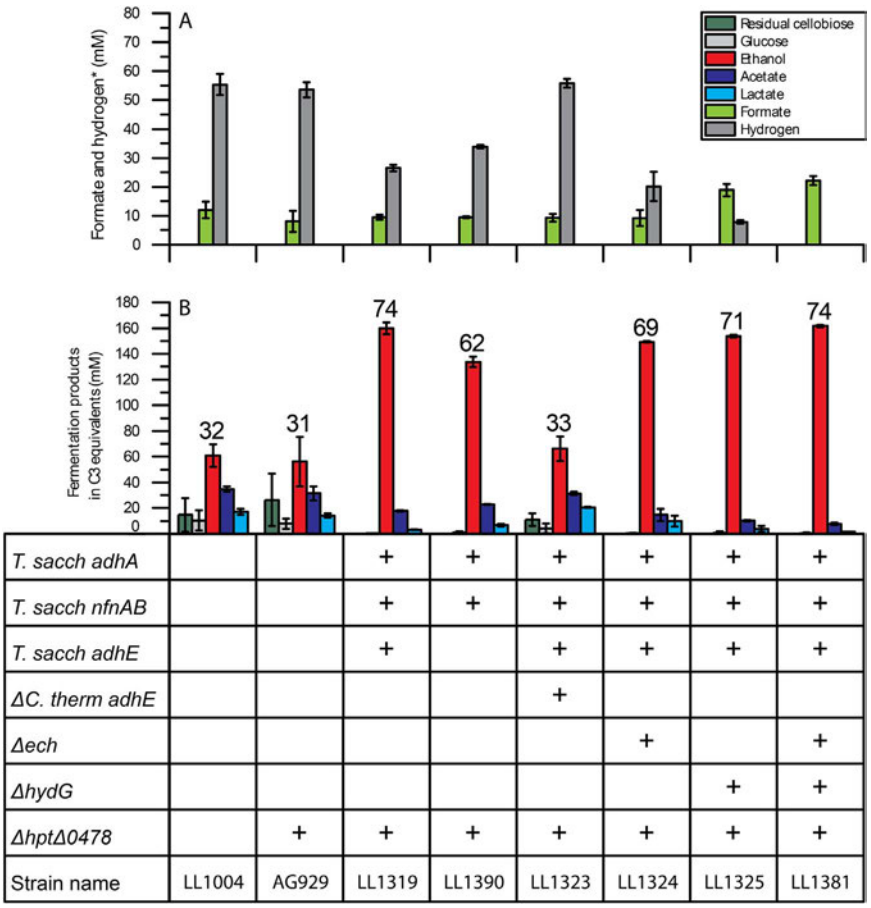

T. sacch adhA			+	+	+	+	+	+
T. sacch nfnAB			+	+	+	+	+	+
T. sacch adhE			+		+	+	+	+
ΔC. therm adhE					+			
Δech						+		+
ΔhydG							+	+
ΔhptΔ0478		+	+	+	+	+	+	+
Strain name	LL1004	AG929	LL1319	LL1390	LL1323	LL1324	LL1325	LL1381

Fig. 5. Hydrogen is reported as millimole of gas per liter of liquid medium. Comparison of hydrogen and formate (**A**) and other fermentation products (**B**) among eight *C. thermocellum* strains; a "+" sign indicates the presence of a genetic modification in the strain. Cultures were grown in sealed serum bottles with 50 mL of MTC-5 medium with 54.4 ± 0.6 mM initial cellobiose (~ 19 g/L) for 72 h at 55 °C with 180 rpm shaking. Colors represent the different measured fermentation products: residual cellobiose (dark green), glucose (light grey), ethanol (red), acetate (dark blue), lactate (light blue), formate (light green), and hydrogen (grey). Error bars represent one standard deviation (n ≥ 3). Values over the ethanol (red) columns indicate the metabolic yield of ethanol as a percentage of theoretical maximum (assuming that a maximum of 2 units of ethanol can be produced from one unit of glucose or glucose equivalent). Raw data and growth rates for the strains are presented in Supplementary information Table S3. * hydrogen is reported as millimole of gas per liter of liquid medium. (For interpretation of the references to color in this figure legend, the reader is referred to the web version of this article)

et al., 2011). However, despite observing the expected decreases in hydrogen production in strains LL1325 (LL1319 *ΔhydG*) and LL1381 (LL1325 *Δech*) (Fig. 5A), we did not observe any significant increase in ethanol production (Fig. 5B), although the increase in formate production in strains LL1325 and LL1381 suggested that electron flux was instead being diverted towards that instead.

The goal of engineering *C. thermocellum* in this work is to produce ethanol from cellulosic biomass. The results presented thus far were from fermentations of a soluble substrate (cellobiose) at relatively low substrate concentrations (20 g/L) (Figs. 2 and 5). We therefore evaluated the fermentation products of two strains, LL1319 and LL1381, at higher substrate concentrations of a cellulosic substrate (60 g/L Avicel microcrystalline cellulose) to determine these two strains' ethanol production performances under more industrially relevant conditions. The decision to evaluate both strains LL1319 and LL1381 was to better determine whether the hydrogenase deletions had any effect on ethanol production in this set of engineered *C. thermocellum* strains.

Both strains LL1319 and LL1381 consumed more than 90% of the 60 g/L Avicel within the first 100 h of fermentation (Fig. 6A and B, respectively). Strain LL1319 achieved a maximum ethanol titer of 326 mM (15.02 g/L)) within 75 h (Fig. 6C) for an ethanol yield of 48% of theoretical maximum, in contrast to the 74% yield observed in 20 g/L cellobiose (Fig. 5). Strain LL1319 also produced 38 mM formate and 54 mM acetate within the same time period; these product titers remained stable for the rest of the fermentation, although there appeared to be a slight decrease in ethanol titer towards the end. Lactate production was minimal until 50 h and accumulated to 26 mM by 75 h; interestingly, there was a second phase of lactate production later in the fermentation between 125 h and 180 h (Fig. 6C). Strain LL1381 reached a maximum ethanol titer of 280 mM (12.90 g/L) within 75 h (Fig. 6D) for an ethanol yield of 39% of theoretical maximum, instead of the 74% observed on 20 g/L cellobiose and also produced more formate (74 mM) and less acetate (30 mM) than LL1319 in the same time period (Fig. 6D). It would therefore seem that the effective elimination of hydrogen production decreased ethanol titer under these fermentation conditions, possibly in part due to a shift of electron flux towards formate production. Overall, the introduced *T. saccharolyticum* ethanol producing pathway improved ethanol titer on high substrate concentrations relative to wild type *C. thermocellum*; for reference, wild type *C. thermocellum* was previously shown to have reached an ethanol titer of 8.01 g/L and 10.43 g/L, on 50.6 g glucose equivalent/L solubilized Avicel and 71.1 g glucose equivalent/L solubilized Avicel, respectively (Holwerda et al., 2014), for their respective ethanol yields of 31% and 29% of theoretical maximum.

3.5. Resequencing analyses of engineered strains

Resequencing of the strains containing the *T. saccharolyticum* ethanol production operon revealed several interesting secondary mutations (additional file 1). We note that strain LL1381 has acquired the previously reported D494G point mutation in the *C. thermocellum adhE* (Biswas et al., 2015; Hon et al., 2016; Zheng et al., 2015) at some point during the deleting of the *ech* complex from strain LL1325. In addition, both strains LL1325 and LL1381 share two mutations: the first is a nucleotide substitution in the acetolactate synthase gene, *Clo1313_0305*, which results in a T105P mutation in the protein. The second shared mutation is a transposon insertion into the *Clo1313_1730* gene, which is annotated as the CheA signal transduction histidine kinase; the transposon insertion results in a premature stop codon in the resulting coding sequence, truncating the protein (see additional file 1).

4. Discussion

In this work, we set out to introduce genes from the high ethanol

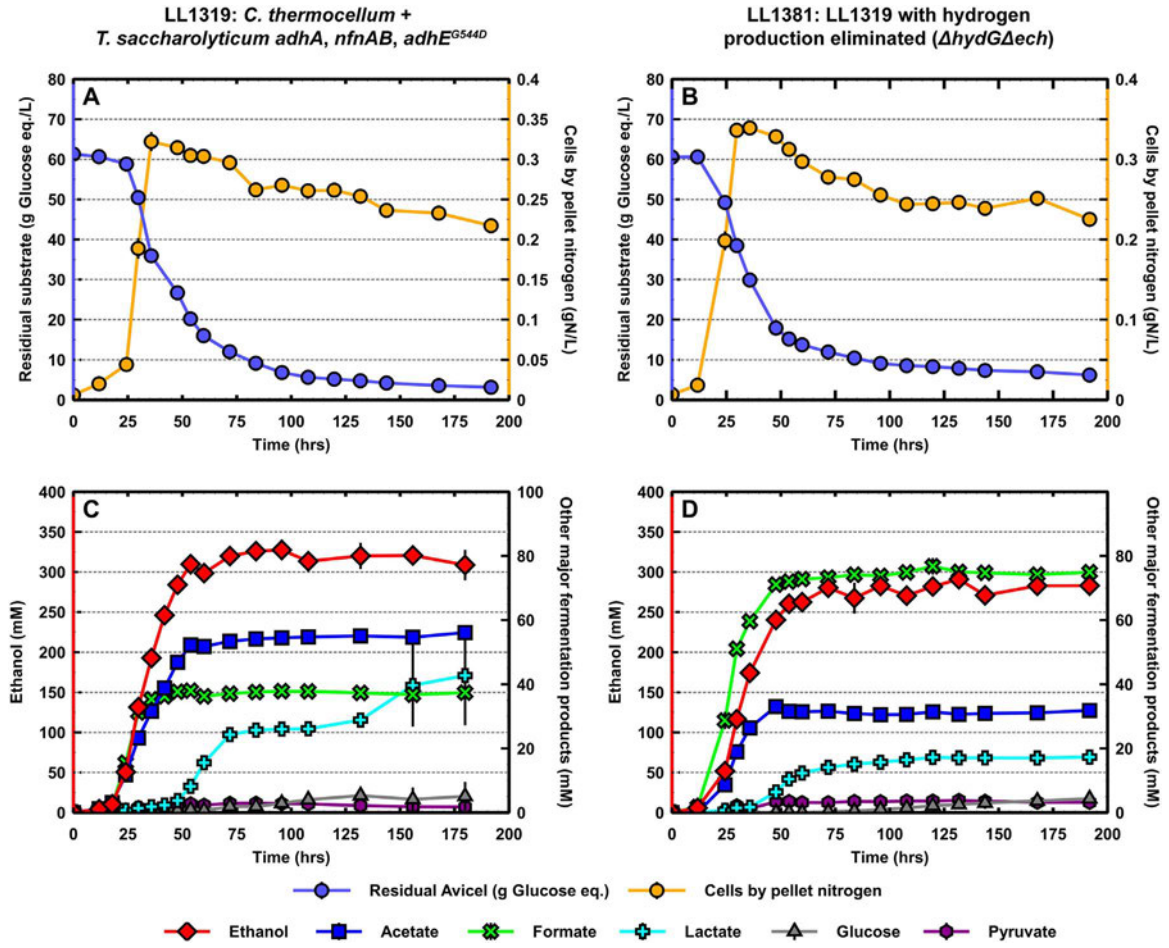

Fig. 6. Substrate utilization as residual cellulose (light blue) and cells as pellet nitrogen (orange) versus fermentation time for strains LL1319 (**A**) and LL1381 (**B**), grown in pH-controlled bioreactors, with 60 g/L crystalline cellulose as the sole carbon source. Major fermentation products – ethanol (red), acetate (dark blue), lactate (light blue), formate (light green), glucose (light grey), and pyruvate (purple) – from the same fermentation runs for strains LL1319 (**C**) and LL1381 (**D**). Error bars on each data point represent mean deviation (n = 2 fermentations). The yield for strain LL1319 is 48% of theoretical maximum; the yield for strain LL1381 is 39% of theoretical maximum. (For interpretation of the references to color in this figure legend, the reader is referred to the web version of this article)

yielding pathway found in engineered *T. saccharolyticum* into *C. thermocellum*. Previous work in *T. saccharolyticum* identified the NADPH-dependent alcohol dehydrogenase, *adhA*, as having an essential role for high ethanol yield and titer in engineered strains of *T. saccharolyticum* (Zheng et al., 2017). We have observed that *adhA* also has a similar effect in *C. thermocellum* in that introducing it improves ethanol yield significantly, but not to levels achieved by *T. saccharolyticum*. Similarly, *nfnAB* was found to be important in engineered *T. saccharolyticum* (Lo et al., 2015b) for high ethanol yield. We observed that *T. saccharolyticum nfnAB* appears to work together with *T. saccharolyticum adhA* to further improve ethanol production; the ability of the NfnAB complex to generate NADPH from NADH and reduced ferredoxin likely explains the synergistic effect of its co-expression with *adhA* (Lo et al., 2015b) in that it replenishes the NADPH pool that the AdhA protein uses to reduce acetaldehyde to ethanol. Despite the fact that the *T. saccharolyticum adhE*^{G544D} gene is essential in engineered *T. saccharolyticum* due to it being the main protein with ALDH activity (Lo et al., 2015a; Zheng et al., 2015), we found that expressing this gene in *C. thermocellum* did not significantly increase total ALDH activity, and only resulted in minor improvements to ethanol yield, suggesting that ALDH activity was primarily due to the native AdhE protein. In addition, the introduced *T. saccharolyticum* AdhE G544D protein on its own (as in strain LL1323) was unable to support ethanol production to high yield and titer even at relatively low substrate loadings (Fig. 5), despite high expression levels of the gene (Fig. 3). One explanation, as indicated by the enzyme activity measurements (Fig. 4), is that the ALDH activity of the introduced AdhE G544D protein is very low in *C. thermocellum*.

The topic of ALDH cofactor specificity is important to discuss. We have previously measured relatively low ALDH activity (< 0.1 U/mg protein) in *T. saccharolyticum* cell extracts. We would have expected a value of greater than about 1 to account for the observed rate of ethanol production. This led us to believe that our ALDH assays were suffering from inhibition or lack of activation. Previously, we had shown that adding ubiquinone-0 improved ALDH activity in *T. saccharolyticum* cell extracts (Lo et al., 2015a; Zheng et al., 2015); however, it did not improve the ALDH activity of AdhE proteins purified from *E. coli*, and in some cases resulted in a large amount of background activity that could not be distinguished from ALDH activity. In the current study, we found that the addition of 5 mM Mg^{2+} to the assay resulted in a large increase in NADH-linked ALDH activity both in purified *T. saccharolyticum* AdhE protein and in cell extract. This suggests that Mg^{2+} is a newly discovered activator for *T. saccharolyticum* AdhE. In strain LL1323, which contains only the *T. saccharolyticum* AdhE G554D (Fig. 4), we found the expected Mg^{2+} stimulation of NADH-ALDH activity. To confirm that the increase in ALDH activity was indeed contributed by AdhE, *T. saccharolyticum* wild-type and G544D AdhE were purified from *E. coli*, and their ALDH cofactor specificity was measured with or without 5 mM Mg^{2+} added to the assay reaction (Fig. S3). The results from measuring the ALDH activities of the purified proteins suggest that NADH is the main cofactor for *T. saccharolyticum* AdhE ALDH activity, and that it requires stimulation by Mg^{2+}. NADPH-linked ALDH activity seemed to be a weaker activity that AdhE gained only after the G544D

Table 3
Comparing ethanol yield and titer, and maximum specific productivity for ethanol for engineered strains of *C. thermocellum*.

Strain	Reference	Ethanol yield on 60 g/L Avicel (% theoretical maximum)	Ethanol titer on 60 g/L Avicel (g/L)	Maximum specific productivity (g/L ethanol /h)
DSM 1313	(Holwerda et al., 2014)	29[a]	10.43[a]	0.31
LL1210	(Tian et al., 2016b)	75	22.40	0.32
LL1319	This study	48	15.02	0.64
LL1381	This study	39	12.90	0.55

[a] Values reported were for an initial substrate concentration of 71.1 g glucose equivalent/L solubilized Avicel.

mutation. After addition of Mg^{2+}, NADPH-linked ALDH activity was 3.2 fold lower than NADH-linked ALDH activity for the G544D enzyme (Fig. S3). This would explain why we did not detect NADPH-linked ALDH activity in LL1323 (expressing the G544D enzyme): NADH-linked ALDH activity was only ~ 0.1 U/mg cell extract, therefore NADPH-linked activity would have been ~ 0.03 U/mg cell extract, and not readily detected by our assay methods. An interesting direction for future work would be to understand how the mutant *T. saccharolyticum* *adhE*^{G544D} supports high ethanol titer in its native organism, or to identify other genes that interact with the acetyl-CoA to ethanol pathway.

Contrary to our expectations, eliminating hydrogen production did not result in further improvement in ethanol yield or titer, as was the case in wild type *C. thermocellum* (Biswas et al., 2015), but instead it resulted in a decrease in ethanol titer; metabolic flux appeared to be re-directed to other fermentation products such as organic acids. We suspect that the deletions in strain LL1381 (strain LL1319 with hydrogenases deleted) have negatively affected electron transfer from ferredoxin to ethanol, as seen by the increase in formate production in strain LL1381 relative to that in strain LL1319. Further studies to both better understand ferredoxin re-oxidation and electron metabolism in engineered *T. saccharolyticum*, as well as efforts to replicate the identified system in engineered *C. thermocellum* may further improve ethanol production in strain LL1319.

Resequencing of strain LL1381 also revealed that it had acquired several secondary mutations, including the D494G mutation in the *C. thermocellum* AdhE protein, which has previously been associated with improved ethanol production. It is possible that any potential benefit that the D494G mutation could have towards ethanol production in strain LL1381 may be offset by the targeted hydrogenase deletions, or by the secondary mutations in the strain, for example the mutations observed in the acetolactate synthase and the putative chemotaxis two-component signal transduction histidine kinase. Understanding how these two mutations affect *C. thermocellum* metabolism and their respective protein functions is an interesting direction for future studies.

In conclusion, we significantly improved ethanol yield, titer, and rate in wild type *C. thermocellum* by introducing just four genes from *T. saccharolyticum*. In particular, the *adhA* gene from *T. saccharolyticum* improved ethanol production in *C. thermocellum* under all conditions. The *nfnAB* and *adhE* ^{G544D} genes resulted in smaller improvements to ethanol production, which were enhanced by the presence of the other introduced *T. saccharolyticum* genes. The ethanol yield of the resulting engineered strain (LL1319) was 74% of theoretical on moderate cellobiose loading, which is similar to the highest values reported in the literature (Table 3, LL1210); the strain also exhibited a faster growth rate (Table S3) than another engineered strain of *C. thermocellum*, LL1210 (Tian et al., 2016b), and also had a higher maximum specific productivity rate of ethanol production (Table 3). However, the ethanol yield of strain LL1319 was lower at high cellulose loading (60 g/L) and as such the maximum titer it has achieved is much lower than that of strain LL1210 (Table 3). The strains from this study still produce unwanted side-products, such as lactate, acetate and formate. It is likely that eliminating the production of these products will further increase ethanol yield and titer.

Although we demonstrated functional expression of 4 genes from *T. saccharolyticum* thought to be essential for high-yield ethanol production, we did not recapitulate the high yield of that strain (~ 90% of the theoretical maximum) (Herring et al., 2016). One possible explanation for the discrepancy is that there are other components from *T. saccharolyticum* that are missing from the introduced system. Another possibility is that the introduced pathway is subject to interference from native *C. thermocellum* host factors. Investigating both of these hypotheses is an interesting direction for future work.

Prior to this work, all of the strains with deletions of the HydG hydrogenase maturation protein were descended from a single strain (LL350), which contained a point mutation in the AdhE protein (D494G) which increased NADPH-ADH activity (Biswas et al., 2015; Zheng et al., 2015). It is possible that the AdhE point mutation plays an important role in the increase in ethanol yield observed in that strain. This interpretation is also supported by recent work showing that re-introduction of the D494G point mutation in AdhE in *C. thermocellum* increased ethanol yield by 50% (Zheng et al., 2015). Interestingly, we acquired the same D494G mutation in our new hydrogenase deletion strain LL1381, suggesting that NADPH-ADH activity is important in the absence of hydrogenases.

Overall, it would suggest that the introduction of NADPH-ADH activity – either by spontaneous mutation of *adhE* (Argyros et al., 2011; Biswas et al., 2015), targeted mutation of *adhE* (Hon et al., 2016; Lo et al., 2015a) or introduction of heterologous *adh* genes (this work) – has been a key factor in the success of these engineering approaches, and may explain why all of them show a similar improvement in ethanol yield of about 50% (vs wild type).

Acknowledgements

We thank Johannes P. van Dijken for useful discussions.

The BioEnergy Science Center is a U.S. Department of Energy Bioenergy Research Center supported by the Office of Biological and Environmental Research (Grant no. DE-AC05-00OR22725) in the DOE Office of Science.

Resequencing was performed by the Department of Energy Joint Genome Institute, a DOE Office of Science User Facility, and is supported by the Office of Science of the U.S. Department of Energy under contract number DE-AC02-05CH11231.

Lee R. Lynd is a founder of the Enchi Corporation, which has a financial interest in *Clostridium thermocellum*.

Appendix A. Supporting information

Supplementary data associated with this article can be found in the online version at http://dx.doi.org/10.1016/j.ymben.2017.06.011.

References

Argyros, D.A., Tripathi, S.A., Barrett, T.F., Rogers, S.R., Feinberg, L.F., Olson, D.G., Foden, J.M., Miller, B.B., Lynd, L.R., Hogsett, D.A., Caiazza, N.C., 2011. High ethanol titers from cellulose by using metabolically engineered thermophilic, anaerobic microbes. Appl. Environ. Microbiol. 77, 8288–8294. http://dx.doi.org/10.1128/AEM.00646-11.

Biswas, R., Prabhu, S., Lynd, L.R., Guss, A.M., 2014. Increase in ethanol yield via elimination of lactate production in an ethanol-tolerant mutant of *Clostridium thermocellum*. PLoS One 9, 1–7. http://dx.doi.org/10.1371/journal.pone.0086389.

Biswas, R., Zheng, T., Olson, D.G., Lynd, L.R., Guss, A.M., Wilson, C.M., Zheng, T., Giannone, R.J., Dawn, M., Olson, D.G., Lynd, L.R., Guss, A.M., 2015. Elimination of hydrogenase active site assembly blocks H_2 production and increases ethanol yield in *Clostridium thermocellum*. Biotechnol. Biofuels 8, 8. http://dx.doi.org/10.1186/s13068-015-0204-4.

Deng, Y., Olson, D.G., Zhou, J., Herring, C.D., Shaw, A.J., Lynd, L.R., 2013. Redirecting carbon flux through exogenous pyruvate kinase to achieve high ethanol yields in

Clostridium thermocellum. Metab. Eng. 15, 151–158. http://dx.doi.org/10.1016/j.ymben.2012.11.006.

Dien, B.S., Cotta, M.A., Jeffries, T.W., 2003. Bacteria engineered for fuel ethanol production: current status. Appl. Microbiol. Biotechnol. 63, 258–266. http://dx.doi.org/10.1007/s00253-003-1444-y.

Espah Borujeni, A., Channarasappa, A.S., Salis, H.M., 2014. Translation rate is controlled by coupled trade-offs between site accessibility, selective RNA unfolding and sliding at upstream standby sites. Nucleic Acids Res. 42, 2646–2659. http://dx.doi.org/10.1093/nar/gkt1139.

Gibson, D.G., 2011. Enzymatic assembly of overlapping DNA fragments. Methods Enzymol. 498, 349–361. http://dx.doi.org/10.1016/B978-0-12-385120-8.00015-2.

Guss, A.M., Olson, D.G., Caiazza, N.C., Lynd, L.R., 2012. Dcm methylation is detrimental to plasmid transformation in *Clostridium thermocellum*. Biotechnol. Biofuels 5, 30. http://dx.doi.org/10.1186/1754-6834-5-30.

Herring, C.D., Kenealy, W.R., Shaw, A.J., Covalla, S.F., Olson, D.G., Zhang, J., Ryan Sillers, W., Tsakraklides, V., Bardsley, J.S., Rogers, S.R., Thorne, P.G., Johnson, J.P., Foster, A., Shikhare, I.D., Klingeman, D.M., Brown, S.D., Davison, B.H., Lynd, L.R., Hogsett, D.A., 2016. Strain and bioprocess improvement of a thermophilic anaerobe for the production of ethanol from wood. Biotechnol. Biofuels 9, 125. http://dx.doi.org/10.1186/s13068-016-0536-8.

Holwerda, E.K., Ellis, L.D., Lynd, L.R., 2013. Development and evaluation of methods to infer biosynthesis and substrate consumption in cultures of cellulolytic microorganisms. Biotechnol. Bioeng. 110, 2380–2388. http://dx.doi.org/10.1002/bit.24915.

Holwerda, E.K., Hirst, K.D., Lynd, L.R., 2012. A defined growth medium with very low background carbon for culturing *Clostridium thermocellum*. J. Ind. Microbiol. Biotechnol. 39, 943–947. http://dx.doi.org/10.1007/s10295-012-1091-3.

Holwerda, E.K., Thorne, P.G., Olson, D.G., Amador-Noguez, D., Engle, N.L., Tschaplinski, T.J., van Dijken, J.P., Lynd, L.R., 2014. The exometabolome of *Clostridium thermocellum* reveals overflow metabolism at high cellulose loading. Biotechnol. Biofuels 7, 155. http://dx.doi.org/10.1186/s13068-014-0155-1.

Hon, S., Lanahan, A.A., Tian, L., Giannone, R.J., Hettich, R.L., Olson, D.G., Lynd, L.R., 2016. Development of a plasmid-based expression system in *Clostridium thermocellum* and its use to screen heterologous expression of bifunctional alcohol dehydrogenases (*adhEs*). Metab. Eng. Commun. 3, 120–129. http://dx.doi.org/10.1016/j.meteno.2016.04.001.

Kannuchamy, S., Mukund, N., Saleena, L.M., 2016. Genetic engineering of *Clostridium thermocellum* DSM1313 for enhanced ethanol production. BMC Biotechnol. 16, 34. http://dx.doi.org/10.1186/s12896-016-0260-2.

Livak, K.J., Schmittgen, T.D., 2001. Analysis of relative gene expression data using real-time quantitative PCR and the $2^{-\Delta\Delta C}_{T}$ method. Methods 25, 402–408. http://dx.doi.org/10.1006/meth.2001.1262.

Lo, J., Olson, D.G., Murphy, S.J.-L., Tian, L., Hon, S., Lanahan, A., Guss, A.M., Lynd, L.R., 2016. Engineering electron metabolism to increase ethanol production in *Clostridium thermocellum*. Metab. Eng. 39, 71–79. http://dx.doi.org/10.1016/j.ymben.2016.10.018.

Lo, J., Zheng, T., Hon, S., Olson, D.G., Lynd, L.R., 2015a. The bifunctional alcohol and aldehyde dehydrogenase gene, *adhE*, is necessary for ethanol production in *Clostridium thermocellum* and *Thermoanaerobacterium saccharolyticum*. J. Bacteriol. 197, 1386–1393. http://dx.doi.org/10.1128/JB.02450-14.

Lo, J., Zheng, T., Olson, D.G., Ruppertsberger, N., Tripathi, S.A., Guss, A.M., Lynd, L.R., 2015b. Deletion of *nfnAB* in *Thermoanaerobacterium saccharolyticum* and its effect on metabolism. J. Bacteriol. 197, 2920–2929. http://dx.doi.org/10.1128/JB.00347-15.

Lynd, L.R., Weimer, P.J., Zyl, W.H. Van, Pretorius, I.S., 2002. Microbial cellulose utilization: fundamentals and biotechnology. Microbiol. Mol. Biol. Rev. 66, 506–577. http://dx.doi.org/10.1128/MMBR.66.3.506.

Olson, D.G., Hörl, M., Fuhrer, T., Cui, J., Zhou, J., Maloney, M.I., Amador-Noguez, D., Tian, L., Sauer, U., Lynd, L.R., 2017. Glycolysis without pyruvate kinase in *Clostridium thermocellum*. Metab. Eng. 39, 169–180. http://dx.doi.org/10.1016/j.ymben.2016.11.011.

Olson, D.G., Lynd, L.R., 2012a. Transformation of *Clostridium thermocellum* by electroporation., 1st ed, Methods in Enzymology. Elsevier Inc. ⟨http://dx.doi.org/10.1016/B978-0-12-415931-0.00017-3⟩.

Olson, D.G., Lynd, L.R., 2012b. Computational design and characterization of a temperature-sensitive plasmid replicon for gram positive thermophiles. J. Biol. Eng. 6. http://dx.doi.org/10.1186/1754-1611-6-5.

Olson, D.G., Maloney, M., Lanahan, A.A., Hon, S., Hauser, L.J., Lynd, L.R., 2015a. Identifying promoters for gene expression in *Clostridium thermocellum*. Metab. Eng. Commun. 2, 23–29. http://dx.doi.org/10.1016/j.meteno.2015.03.002.

Olson, D.G., McBride, J.E., Shaw, A.J., Lynd, L.R., 2012. Recent progress in consolidated bioprocessing. Curr. Opin. Biotechnol. 23, 396–405. http://dx.doi.org/10.1016/j.copbio.2011.11.026.

Olson, D.G., Sparling, R., Lynd, L.R., 2015b. Ethanol production by engineered thermophiles. Curr. Opin. Biotechnol. 33, 130–141. http://dx.doi.org/10.1016/j.copbio.2015.02.006.

Papanek, B., Biswas, R., Rydzak, T., Guss, A.M., 2015. Elimination of metabolic pathways to all traditional fermentation products increases ethanol yields in *Clostridium thermocellum*. Metab. Eng. 32, 49–54. http://dx.doi.org/10.1016/j.ymben.2015.09.002.

Paye, J.M.D., Guseva, A., Hammer, S.K., Gjersing, E., Davis, M.F., Davison, B.H., Olstad, J., Donohoe, B.S., Nguyen, T.Y., Wyman, C.E., Pattathil, S., Hahn, M.G., Lynd, L.R., 2016. Biological lignocellulose solubilization: comparative evaluation of biocatalysts and enhancement via cotreatment. Biotechnol. Biofuels 9, 8. http://dx.doi.org/10.1186/s13068-015-0412-y.

Rydzak, T., Lynd, L.R., Guss, A.M., 2015. Elimination of formate production in *Clostridium thermocellum*. J. Ind. Microbiol. Biotechnol. http://dx.doi.org/10.1007/s10295-015-1644-3.

Salis, H.M., Mirsky, E.A., Voigt, C.A., 2009. Automated design of synthetic ribosome binding sites to control protein expression. Nat. Biotechnol. 27, 946–950. http://dx.doi.org/10.1038/nbt.1568.

Shaw, A.J., Covalla, S.F., Miller, B.B., Firliet, B.T., Hogsett, D.A., Herring, C.D., 2012. Urease expression in a *Thermoanaerobacterium saccharolyticum* ethanologen allows high titer ethanol production. Metab. Eng. 14, 528–532. http://dx.doi.org/10.1016/j.ymben.2012.06.004.

Shaw, A.J., Podkaminer, K.K., Desai, S.G., Bardsley, J.S., Rogers, S.R., Thorne, P.G., Hogsett, D.A., Lynd, L.R., 2008. Metabolic engineering of a thermophilic bacterium to produce ethanol at high yield. Proc. Natl. Acad. Sci. USA 105, 13769–13774. http://dx.doi.org/10.1073/pnas.0801266105.

Tian, L., Lo, J., Shao, X., Zheng, T., Olson, D.G., Lynd, R., 2016a. Ferredoxin:NAD^+ oxidoreductase of *Thermoanaerobaceriums saccharolyticum* and its role in ethanol formation. Appl. Environ. Microbiol. 82, 7134–7141. http://dx.doi.org/10.1128/AEM.02130-16.

Tian, L., Papanek, B., Olson, D.G., Rydzak, T., Holwerda, E.K., Zheng, T., Zhou, J., Maloney, M., Jiang, N., Giannone, R., Hettich, R., Guss, A., Lynd, L., 2016b. Simultaneous achievement of high ethanol yield and titer in *Clostridium thermocellum*. Biotechnol. Biofuels 9, 1–11. http://dx.doi.org/10.1186/s13068-016-0528-8.

Zheng, T., Olson, D.G., Murphy, S.J.-L., Shao, X., Tian, L., Lynd, L.R., 2017. Both *adhE* and a separate NADPH-dependent alcohol dehydrogenase (*adhA*) are necessary for high ethanol production in *Thermoanaerobacterium saccharolyticum*. J. Bacteriol. 199, 1–10. http://dx.doi.org/10.1128/JB.00542-16.

Zheng, T., Olson, D.G., Tian, L., Bomble, Y.J., Himmel, M.E., Lo, J., Hon, S., Shaw, A.J., van Dijken, J.P., Lynd, L.R., 2015. Cofactor specificity of the bifunctional alcohol and aldehyde dehydrogenase (AdhE) in wild-type and mutants of *Clostridium thermocellum* and *Thermoanaerobacterium saccharolyticum*. J. Bacteriol. 197, 2610–2619. http://dx.doi.org/10.1128/JB.00232-15.

Zheng, Y., Kahnt, J., Kwon, I.H., Mackie, R.I., Thauer, R.K., 2014. Hydrogen formation and its regulation in *Ruminococcus albus*: involvement of an electron-bifurcating [FeFe]-hydrogenase, of a non electron-bifurcating [FeFe]-hydrogenase and of a putative hydrogen-sensing [FeFe]-hydrogenase. J. Bacteriol. 196, 3840–3852. http://dx.doi.org/10.1128/JB.02070-14.

Zhou, J., Olson, D.G., Lanahan, A.A., Tian, L., Murphy, S.J.-L., Lo, J., Lynd, L.R., 2015. Physiological roles of pyruvate ferredoxin oxidoreductase and pyruvate formate-lyase in *Thermoanaerobacterium saccharolyticum* JW/SL-YS485. Biotechnol. Biofuels 8, 138. http://dx.doi.org/10.1186/s13068-015-0304-1.